

Supporting Information

Atomically Accurate Structural Tailoring of Thiocalix[4]arene-Protected Copper(II)-Based Metallamacrocycles

Wen-Lei Mu,^{a†} Linlin Wu,^{a†} Wei-Dong Yu,^{b*} Xiao-Yi Yi,^a Jun Yan,^a and Chao Liu^{a*}

^a Hunan Provincial Key Laboratory of Chemical Power Sources, College of Chemistry and Chemical Engineering, Central South University, Changsha 410083, Hunan, P. R. China

^b China College of Science, Hunan University of Technology and Business, Changsha 410000, P. R. China

^c Institute of Environmental Research at Greater Bay Area; Key Laboratory for Water Quality and Conservation of the Pearl River Delta, Ministry of Education; Guangzhou Key Laboratory for Clean Energy and Materials, Guangzhou University, Guangzhou 510006, China

Corresponding Authors

*(Chao Liu) E-mail: chaoliu@csu.edu.cn

1. Experimental Section

Materials and Characterization. All reagents were purchased commercially and were not further purified when used. Powder X-ray diffraction (PXRD) analysis were performed on a Rigaku Mini Flex II diffractometer at a 2θ range of $3\text{--}50^\circ$ (5° min^{-1}) with CuK_α radiation ($\lambda = 1.54056 \text{ \AA}$). The solid-state UV/Vis spectra data of the cluster samples were obtained on UV-4000 spectrophotometer. Electrospray ionization mass spectrometry (ESI-MS) were performed on a Bruker Daltonik GmbH (Bruker, Germany). Thermogravimetric (TGA) patterns were recorded on a Mettler Toledo TGA/SDTA 851e analyzer in a N₂ atmosphere. FT-IR spectra using KBr pellets were taken on a Bruker Vertex 70 Spectrometer.

Synthesis for compound $\{\text{HNa}_2\text{Cu}_{12}\text{Cl}_3(\text{TC4A})_3(\text{PhPO}_3)_6(\text{H}_2\text{O})_2\} \cdot 9\text{iPrOH} \cdot \{\text{Cu}_{12}\text{L}_3\}$: PhPO₃H₂ (26 mg, 0.16 mmol), TC4A (20mg, 0.03 mmol), CuCl (15mg, 0.15mmol), 3mL isopropanol and 50 μL triethylamine were added to a 25 mL glass bottle. The resulting mixtures were sonicated for 5 min, then were transferred to a preheated oven at 100 °C for 3 days. Red rectangle crystals were obtained after cooling to 25°C (yield: ~30%, based on CuCl).

Synthesis for compound $\{\text{H}_3\text{Cu}_{16}\text{Cl}_3(\text{TC4A})_4(\text{PhPO}_3)_8\} \cdot 5\text{DMF} \cdot \{\text{Cu}_{16}\text{L}_4\}$: PhPO₃H₂ (26 mg, 0.16 mmol), TC4A (20mg, 0.03 mmol), CuCl (15mg,0.15mmol), 50 μL triethylamine, 2 mL isopropanol and 1 mL DMF were added to a 25 mL glass bottle. After stirring for 10 min, the resulting mixtures were transferred to a preheated oven at 100°C for 3 days. Yellow rhomboid crystals were obtained after cooling to 25°C (yield: ~37%, based on CuCl).

Synthesis for compound $\{\text{H}_5\text{NaCu}_{12}(\text{TC4A})_4(\text{PhPO}_3)_8(\text{Sa})\} \cdot 7.5\text{iPrOH} \cdot \{\text{Cu}_{12}\text{L}_3\text{-Sa}\}$: PhPO₃H₂ (26 mg, 0.16 mmol), H₂Sa (15 mg, 0.13 mmol), TC4A (20mg, 0.03 mmol), CuCl (15 mg, 0.15mmol), isopropanol (2mL), DMF(1mL) and triethylamine (50 μL) were added to a 25 mL glass bottle and transferred to a preheated oven at 120°C for 3 days. A large amount of yellow rectangle crystal was obtained after cooling to 25°C (yield: ~27%, based on CuCl).

Synthesis for compound $\{\text{Cu}_{16}\text{Cl}_4(\text{TC4A})_4(\text{PhPO}_3)_6(\text{Sa})_2\} \cdot 9\text{DMF} \cdot \{\text{Cu}_{16}\text{L}_4\text{-Sa}\}$: PhPO₃H₂ (26 mg, 0.16 mmol), H₂Sa (15 mg, 0.13 mmol), TC4A (20mg, 0.03 mmol), CuCl (15mg,0.15mmol), 2 mL isopropanol and 1mL DMF were added to a 10mL glass bottle, and then added with 100 μL Ti(O*i*Pr)₄, 100 mL and 50 μL triethylamine. After stirring for 10 min, the resulting mixtures were transferred to a preheated oven at 80 °C for 3 days. Brownish yellow block crystals were obtained after cooling to 25°C (yield: ~8%, based on CuCl).

X-ray Crystal Structure Determination. Single crystal diffraction data was collected on Bruker D8 Venture diffractometer with liquid metal Ga K α radiation. The structures were solved using intrinsic phasing methods in ShelXT program and then refined by full-matrix least-squares on F2 using ShelXL-2014 in Olex² program. The hydrogen atoms were introduced at their geometric positions and refined as riding atom, and the positions of non-hydrogen atoms were refined with anisotropic displacement parameters during the final cycles. Due to the rotation disorder of tert-butyl groups, in all cases the

ISOR, DELU and SIMU constraints were necessary to achieve convergence. For all the clusters, the highly disordered solvent molecules in the crystal structures were removed with the SQUEEZE program in PLATON and their possible formulas were proposed based on the SQUEEZE and TGA results. A summary of the crystallographic data for the reported clusters is listed in Table S1. CCDC 2225573-2225576 contain the crystallographic data herein.

Typical procedure for the oxidation of desulfurization. The catalytic reactions were carried out with sulfide (0.7 mmol), catalyst (5mg, 1.09 μ mol for Cu_{12}L_3 , 0.98 μ mol for $\text{Cu}_{12}\text{L}_3\text{-Sa}$, 0.9 μ mol for Cu_{16}L_4), H_2O_2 (30%, 200 μ L), and 5 mL solvent. The reaction was stirred at 50°C at a certain time. After reaction, the mixtures were analysed by gas chromatography (GC) and ^1H NMR. The catalysts were collected by filtration and washed with CH_3OH , and reused for the next cycle.

DFT calculations were performed with Gaussian16 package.^[1] B3LPY functional was used for calculations.^[2-4] The Lanl2dz basis set was used to describe The effective core potentials (ECPs) of Lanl2dz used to describe Cu, Cl, S and P atoms, with polarization functions for Cu ($\zeta_f = 0.640$), Cl ($\zeta_d = 0.640$), S ($\zeta_d = 0.503$), and P ($\zeta_d = 0.387$) being added.^[5-7] For all of the remaining atoms, the basis set 6-31G* was adopted to ensure accuracy.^[8,9]

Reference:

- [1] Frisch, M. J.; Trucks, G. W.; Schlegel, H. B.; Scuseria, G. E.; Robb, M. A.; Cheeseman, J. R.; Scalmani, G.; Barone, V.; Petersson, G. A.; Nakatsuji, H.; Li, X.; Caricato, M.; Marenich, A. V.; Bloino, J.; Janesko, B. G.; Gomperts, R.; Mennucci, B.; Hratchian, H. P.; Ortiz, J. V.; Izmaylov, A. F.; Sonnenberg, J. L.; Williams; Ding, F.; Lipparini, F.; Egidi, F.; Goings, J.; Peng, B.; Petrone, A.; Henderson, T.; Ranasinghe, D.; Zakrzewski, V. G.; Gao, J.; Rega, N.; Zheng, G.; Liang, W.; Hada, M.; Ehara, M.; Toyota, K.; Fukuda, R.; Hasegawa, J.; Ishida, M.; Nakajima, T.; Honda, Y.; Kitao, O.; Nakai, H.; Vreven, T.; Throssell, K.; Montgomery Jr., J. A.; Peralta, J. E.; Ogliaro, F.; Bearpark, M. J.; Heyd, J. J.; Brothers, E. N.; Kudin, K. N.; Staroverov, V. N.; Keith, T. A.; Kobayashi, R.; Normand, J.; Raghavachari, K.; Rendell, A. P.; Burant, J. C.; Iyengar, S. S.; Tomasi, J.; Cossi, M.; Millam, J. M.; Klene, M.; Adamo, C.; Cammi, R.; Ochterski, J. W.; Martin, R. L.; Morokuma, K.; Farkas, O.; Foresman, J. B.; Fox, D. J.: Gaussian 16 Rev. C.01. Wallingford, CT, 2016
- [2] Miehlich, B.; Savin, A.; Stoll, H.; Preuss, H. Results obtained with the correlation energy density functionals of becke and Lee, Yang and Parr. *Chem. Phys. Lett.* **1989**, *157*, 200-206.
- [3] Lee, C.; Yang, W.; Parr, R. G. Development of the Colle-Salvetti correlation-energy formula into a functional of the electron density. *Physical Review B* **1988**, *37*, 785-789.
- [4] Becke, A. D. Density-functional thermochemistry. III. The role of exact exchange. *The Journal of Chemical Physics* **1993**, *98*, 5648-5652.
- [5] Hay, P. J.; Wadt, W. R. Ab initio effective core potentials for molecular calculations. Potentials for K to Au including the outermost core orbitals. *The Journal of Chemical Physics* **1985**, *82*, 299-310.
- [6] Wadt, W. R.; Hay, P. J. Ab initio effective core potentials for molecular calculations. Potentials for main group elements Na to Bi. *The Journal of Chemical Physics* **1985**, *82*, 284-298.
- [7] Hay, P. J.; Wadt, W. R. Ab initio effective core potentials for molecular calculations. Potentials for the transition metal atoms Sc to Hg. *The Journal of Chemical Physics* **1985**, *82*, 270-283.
- [8] Krishnan, R.; Binkley, J. S.; Seeger, R.; Pople, J. A. Self-consistent molecular orbital methods. XX. A basis set for correlated wave functions. *The Journal of Chemical Physics* **1980**, *72*, 650-654.
- [9] McLean, A. D.; Chandler, G. S. Contracted Gaussian basis sets for molecular calculations. I. Second row atoms, Z=11–18. *The Journal of Chemical Physics* **1980**, *72*, 5639-5648.

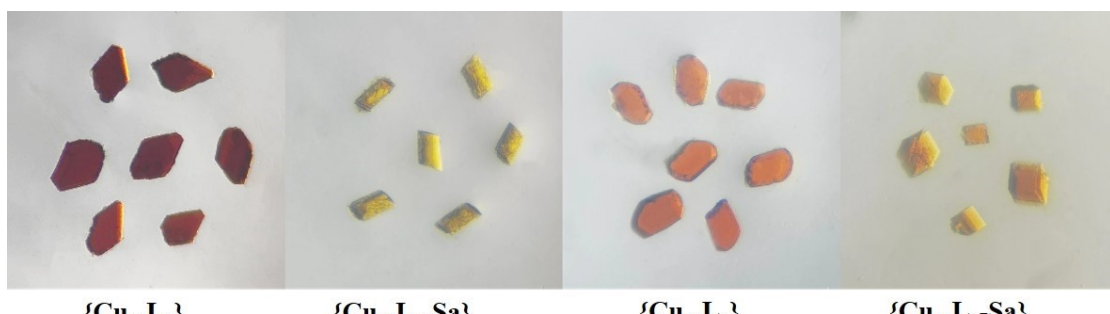


Figure S1. Pictures of fresh crystals separated from the solution.

2. Structure of Compounds

Compounds	Cu₁₂L₃	Cu₁₂L₃-Sa	Cu₁₆L₄	Cu₁₆L₄-Sa
CCDC	2225573	2225574	2225575	2225576
Formula	C ₁₈₃ H ₂₂₅ O ₄₁ Cl ₃ Cu ₁₂ Na ₂ P ₆ S ₁₂	C _{212.5} H _{269.5} Cu ₁₂ O _{53.5} P ₈ S ₁₂	C ₂₂₀ H ₂₄₂ Cl ₃ Cu ₁₆ N ₄ O ₄₄ P ₈ S ₁₆	C ₂₁₆ H ₂₃₈ Cl ₄ Cu ₁₆ O ₄₆ P ₆ S ₁₆
T(K)	150	150	150	150
F _w	4565.97	5074.73	5536.07	5483.49
Crystal system	triclinic	monoclinic	monoclinic	triclinic
Space group	P-1	P2 ₁ /n	P2 ₁ /n	P-1
a, Å	17.190(3)	13.44160(10)	17.160(2)	17.1459(11)
b, Å	25.858(6)	64.1367(5)	33.513(5)	20.4847(15)
c, Å	28.437(6)	25.1780(2)	22.472(3)	22.6894(14)
α/°	66.779(6)	90	90	74.314(2)
β/°	89.744(5)	103.1780(10)	96.721(6)	68.612(2)
γ/°	77.581(6)	90	90	75.244(2)
V/Å ³	11299(4)	21134.4(3)	12834(3)	7034.9(8)
Z	2	4	2	1
ρ _{calcd} /gcm ⁻³)	1.186	1.595	1.440	1.294
μ/mm ⁻¹)	7.448	3.631	8.733	7.896
F(000)	4114.0	10530.0	5700	2808.0
Radiation	GaKα (λ = 1.34139)	Cu Kα (λ = 1.54184)	GaKα (λ = 1.34139)	GaKα (λ = 1.34139)
Data/restraints/pa rameters	36208/592/1979	37280/2383/2880	27914/190/1481	23140/424/1411
2Θ range for data collection/°	8.3 to 102.876	4.538 to 133.202	5.738 to 118.822	5.114 to 102.866
Goof	0.970	1.050	1.058	0.975
R ₁ /wR ₂ (I>2σ(I))	0.1116/0.3019	0.0827/0.2235	0.0664/0.1980	0.0781/0.2132
R ₁ /wR ₂ (all data)	0.1720/0.3462	0.1033/0.2383	0.0827/0.2097	0.1350/0.2457

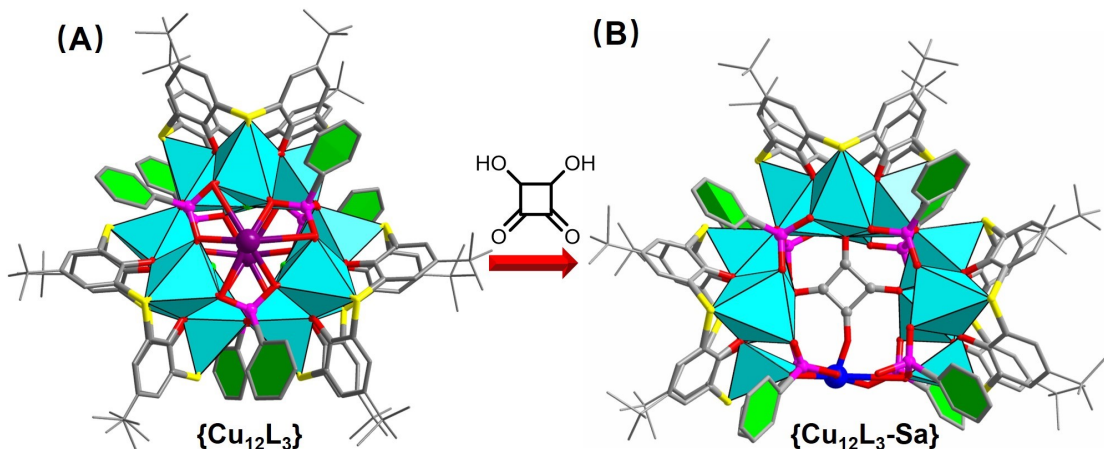


Figure S2. Structure of Cu₁₂L₃ and Cu₁₂L₃-Sa.

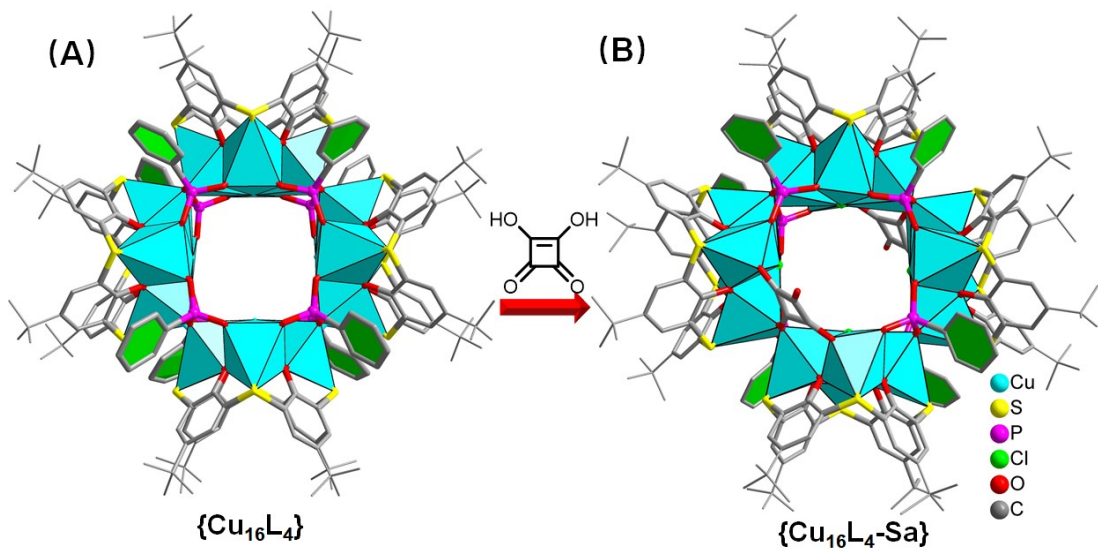


Figure S3. Structure of $Cu_{16}L_4$ and $Cu_{16}L_4\text{-}Sa$.

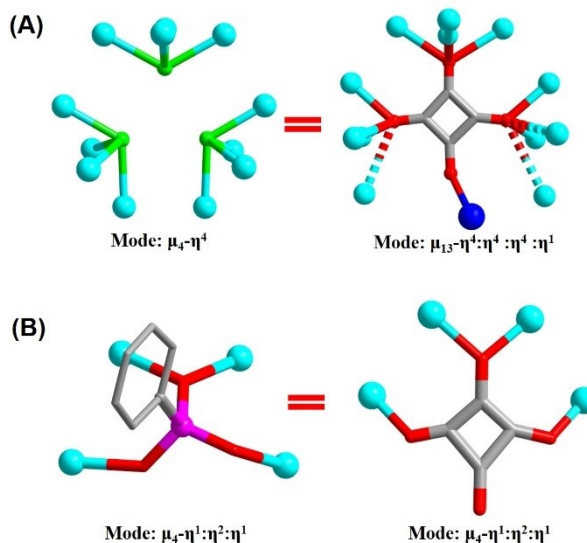


Figure S4. Coordination modes of Cl^- , Sa^{2-} and $PhPO_3^{2-}$ ligands.

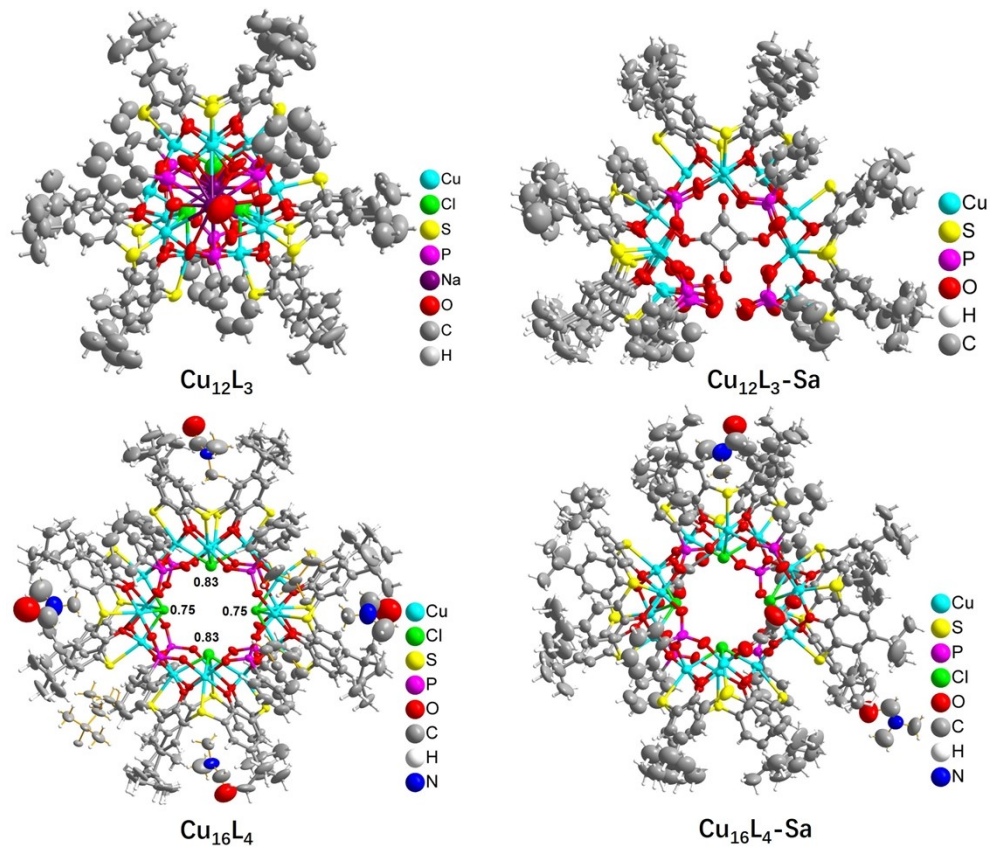


Figure S5. ORTEP representation of the structures.

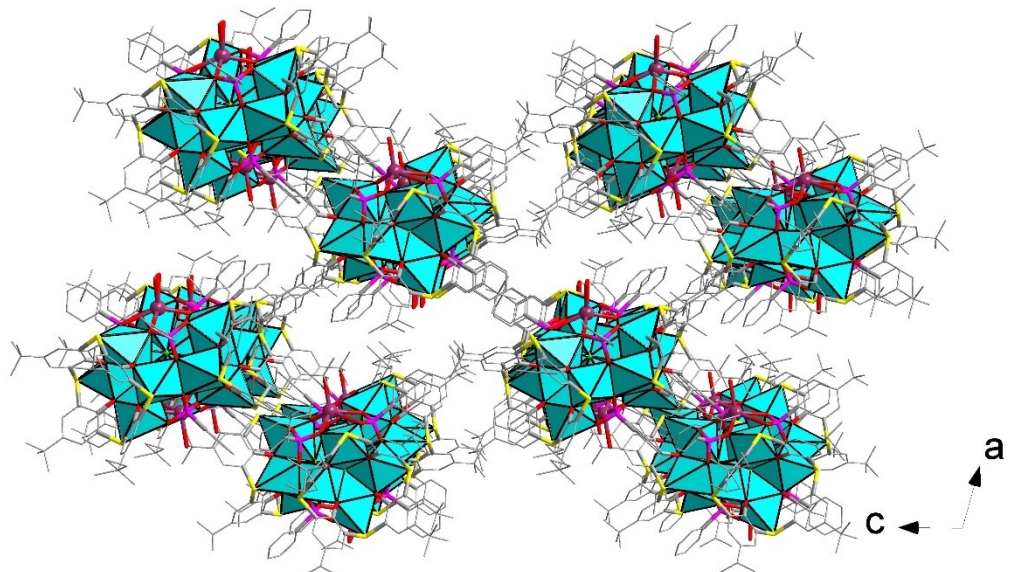


Figure S6. Three-dimensional packing structure of Cu_{12}L_3 .

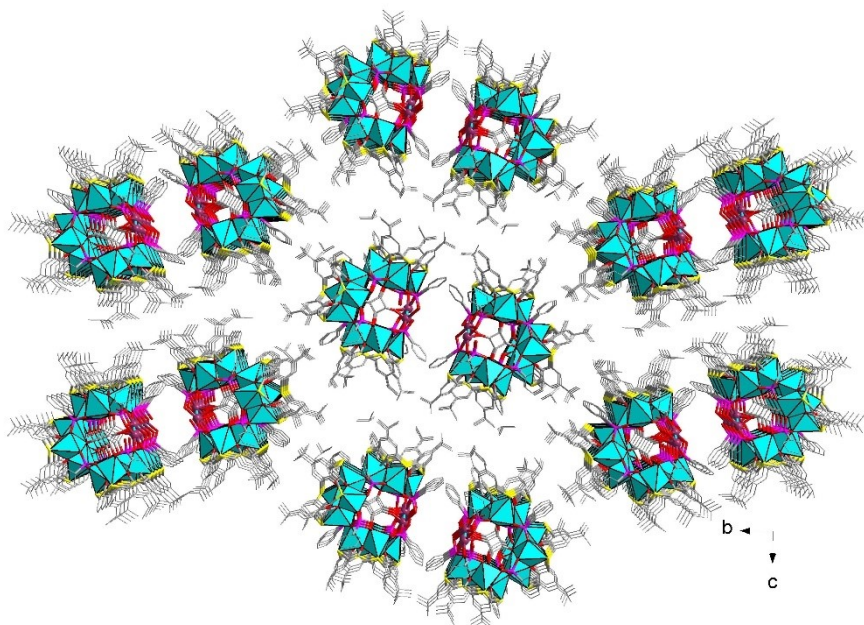


Figure S7. Three-dimensional packing structure of Cu₁₂L₃-Sa.

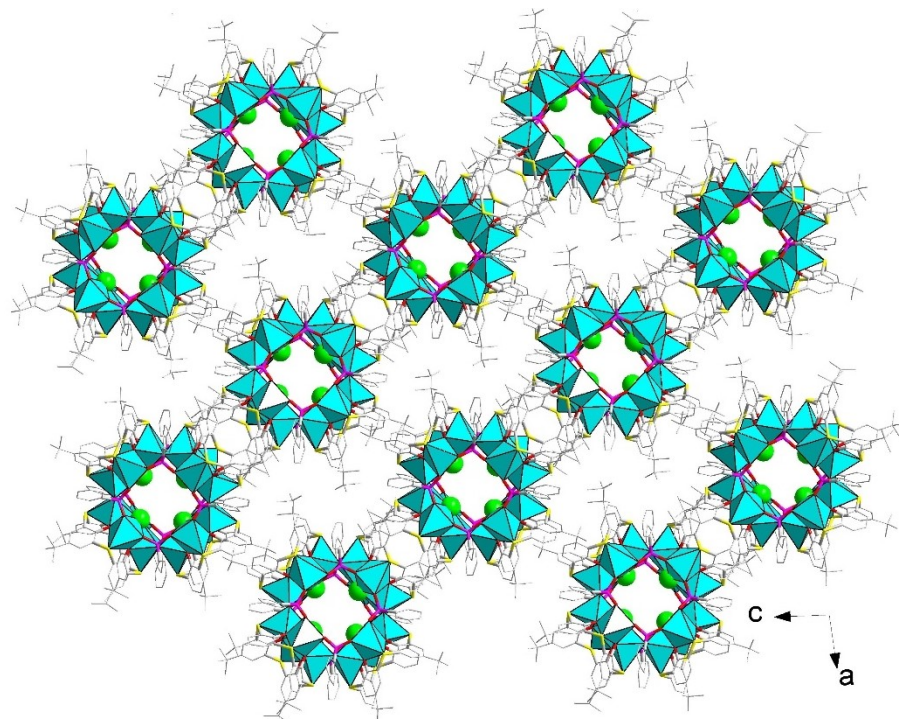


Figure S8. Three-dimensional packing structure of Cu₁₆L₄.

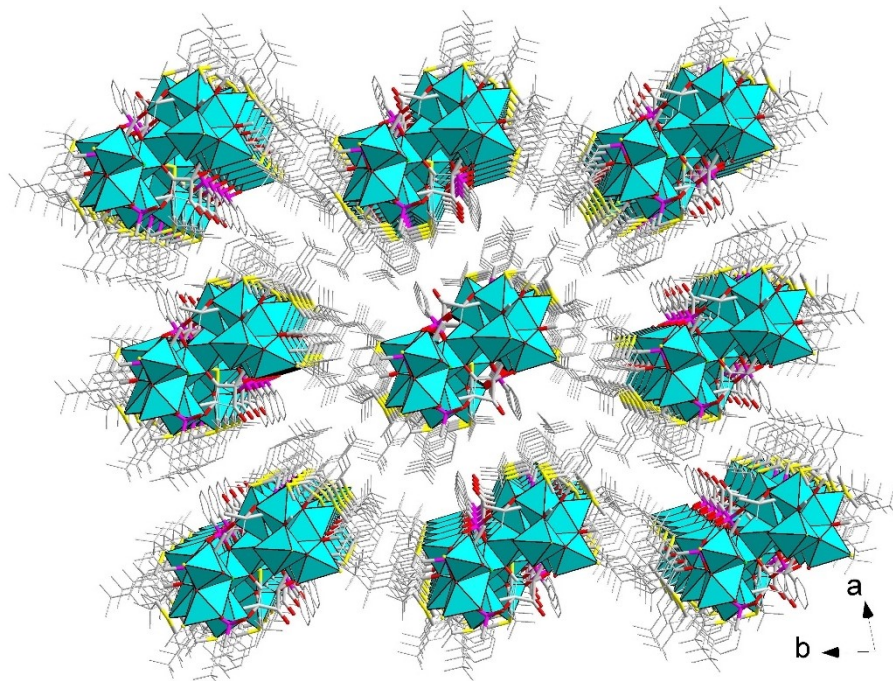


Figure S9. Three-dimensional packing structure of $\text{Cu}_{16}\text{L}_4\text{Sa}$.

3. Powder X-ray Diffraction

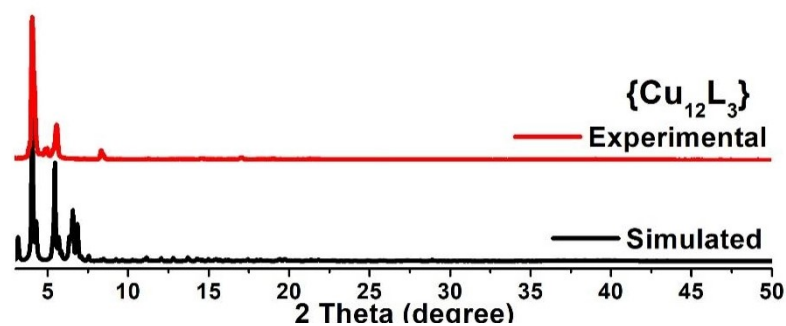


Figure S10. The XRD patterns of Cu_{12}L_3 .

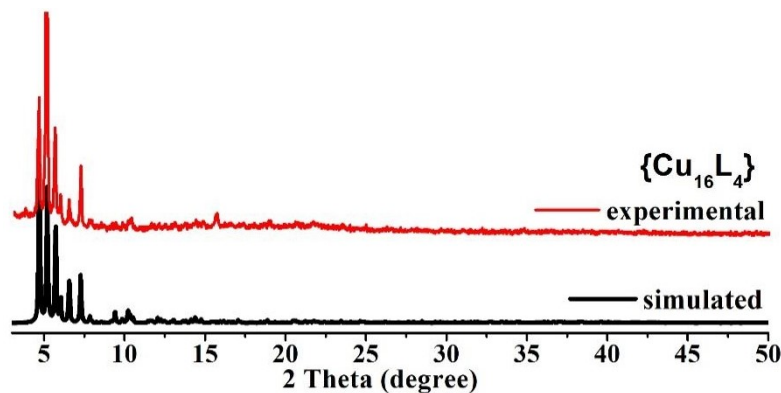


Figure S11. The XRD pattern of Cu_{16}L_4 .

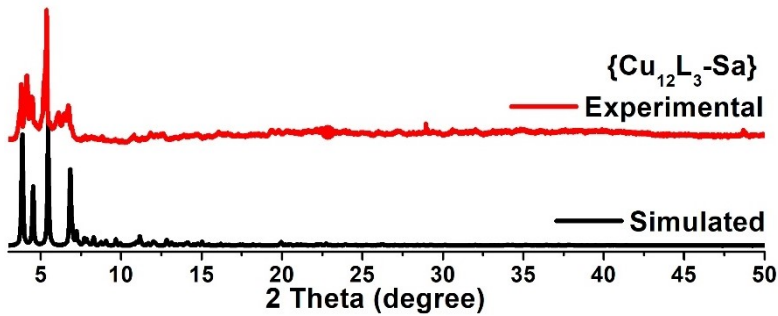


Figure S12. The XRD pattern of $Cu_{12}L_3\text{-Sa}$.

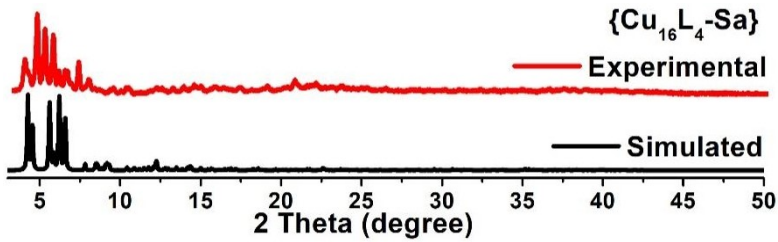


Figure S13. The XRD patterns of $Cu_{16}L_4\text{-Sa}$.

6. Energy Dispersive X-ray (EDX) Spectroscopic Analysis

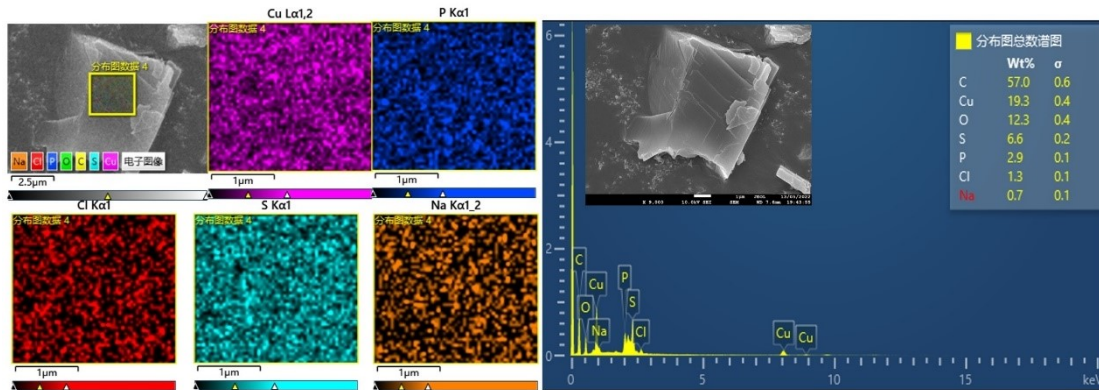


Figure S14. The EDS pattern of $Cu_{12}L_3$.

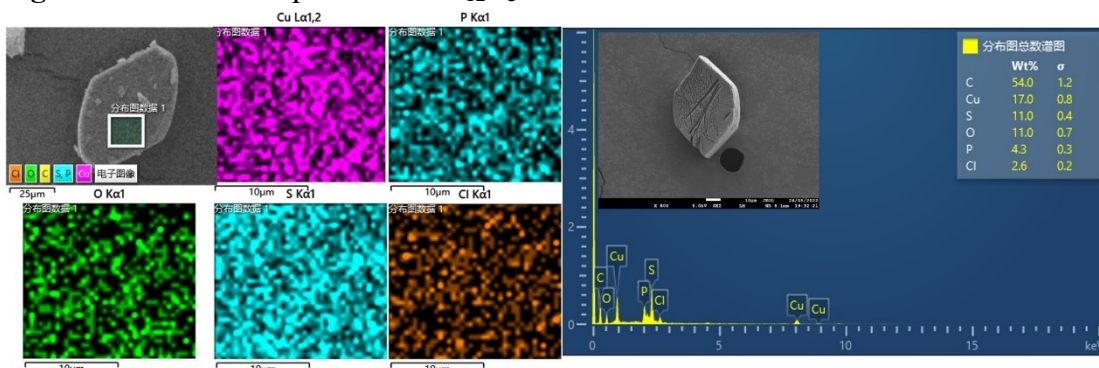


Figure S15. The EDS pattern of $Cu_{16}L_4$.

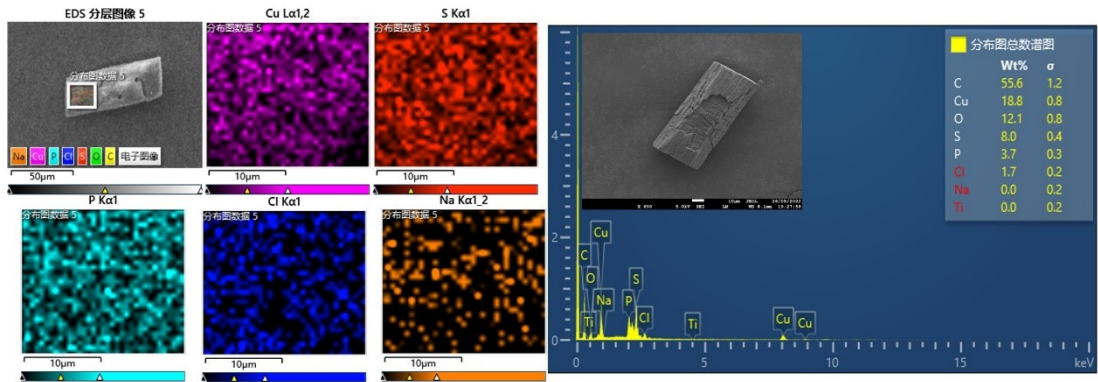


Figure S16. The EDS pattern of $\text{Cu}_{12}\text{L}_3\text{-Sa}$.

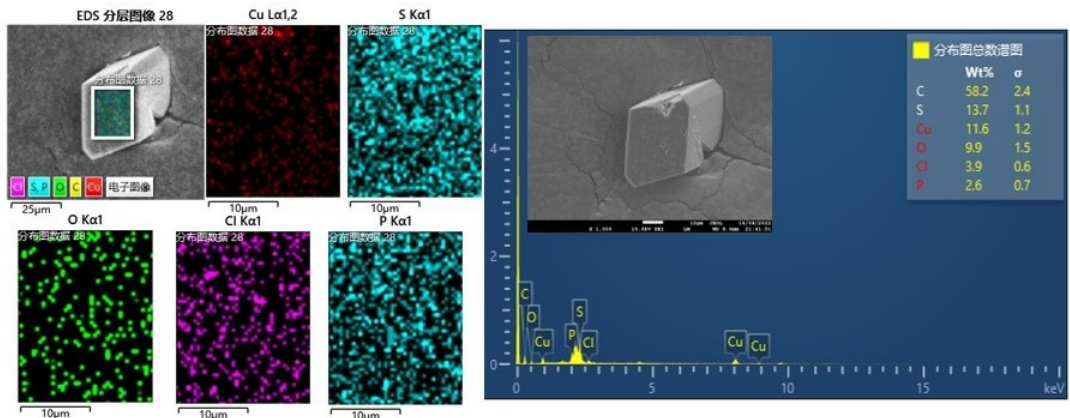


Figure S17. The EDS pattern of $\text{Cu}_{16}\text{L}_4\text{-Sa}$.

7. TG-Measurement

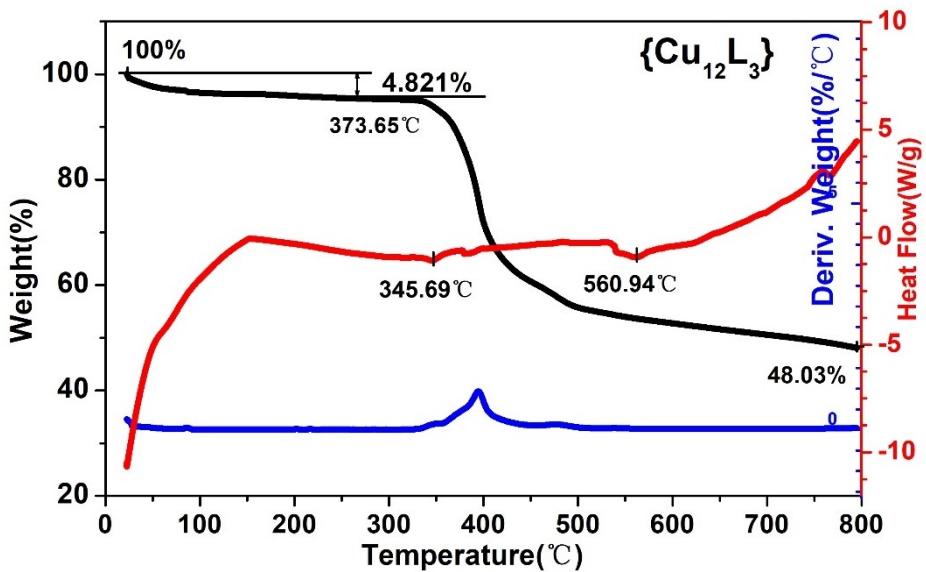


Figure S18. The TGA and DSC curves of Cu_{12}L_3 .

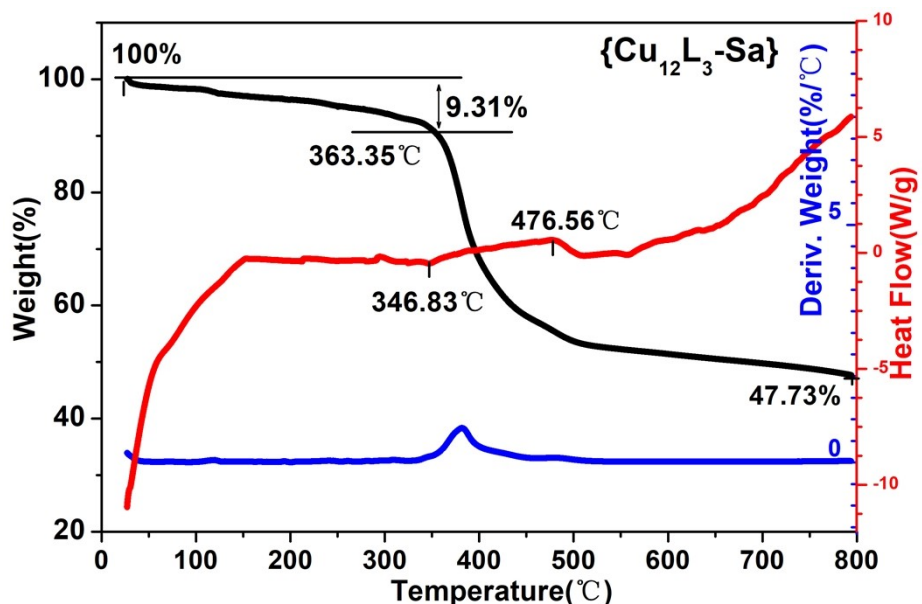


Figure S19. The TGA and DSC curves of $Cu_{12}L_3\text{-Sa}$.

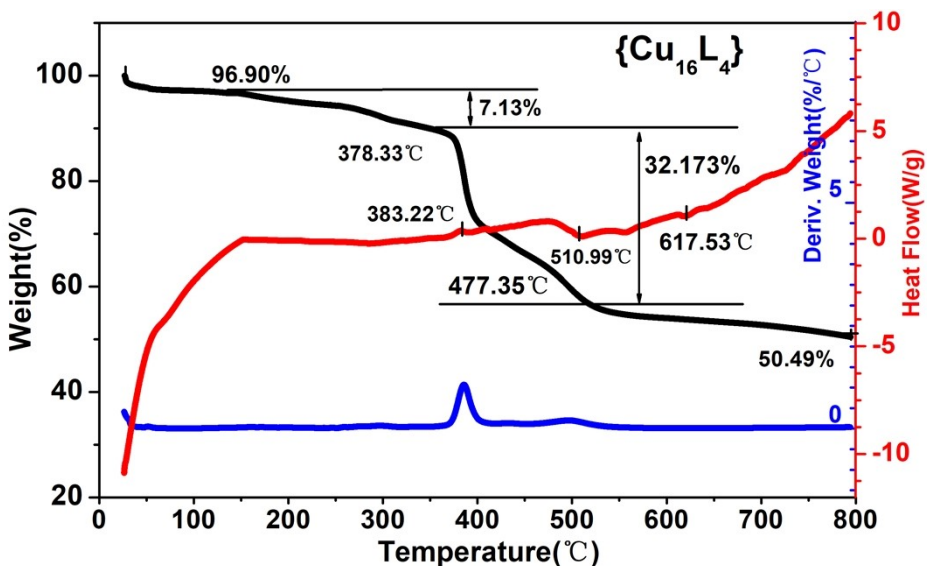


Figure S20. The TGA and DSC curves of $Cu_{16}L_4$.

8. IR Spectra

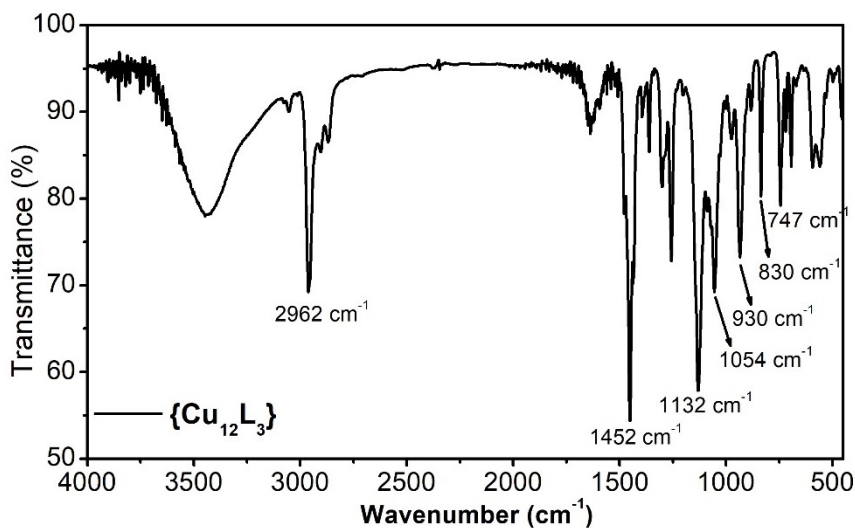


Figure S21. IR spectrum of crystal sample of Cu_{12}L_3 .

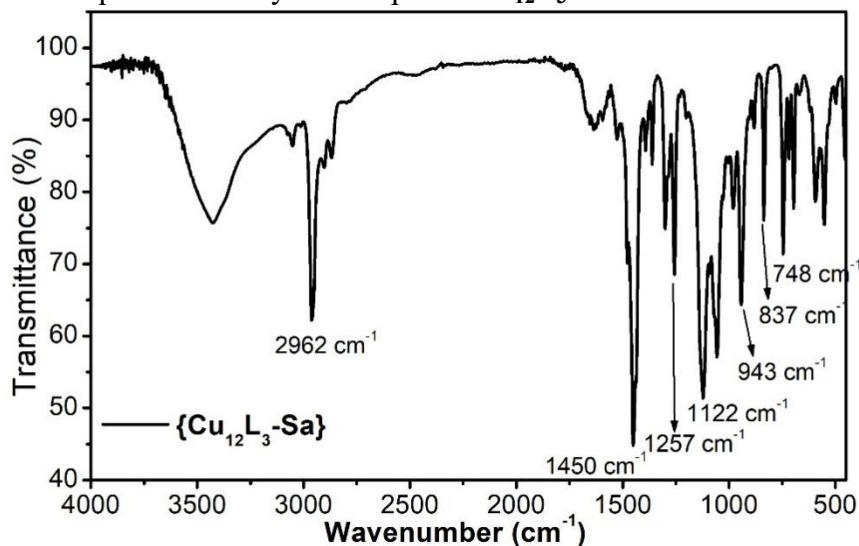


Figure S22. IR spectrum of crystal sample of $\text{Cu}_{12}\text{L}_3\text{-Sa}$.

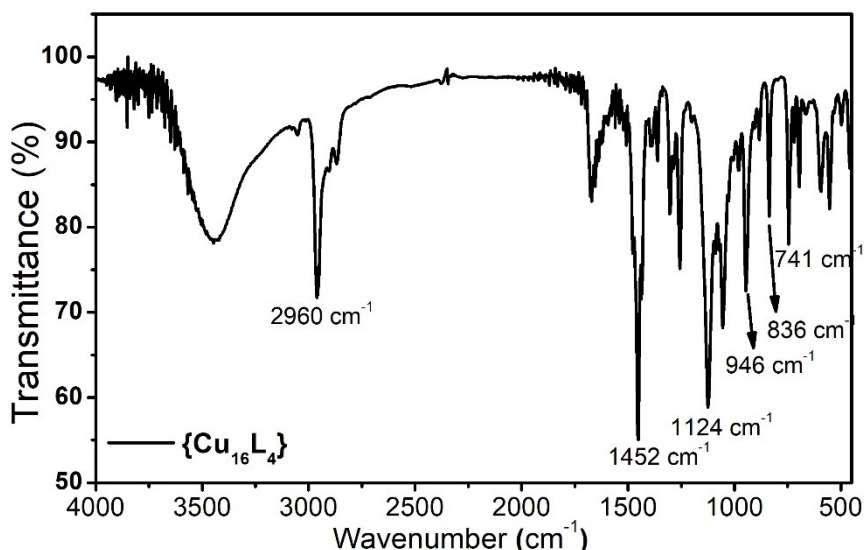


Figure S23. IR spectrum of crystal sample of Cu_{16}L_4 .

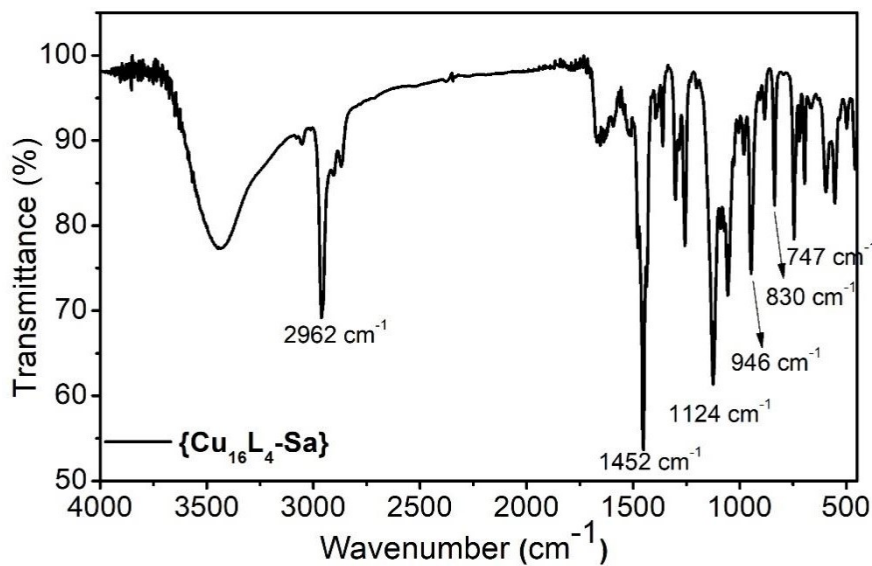


Figure S24. IR spectrum of crystal sample of $\text{Cu}_{16}\text{L}_4\text{-Sa}$.

9. ESI-MS Measurements.

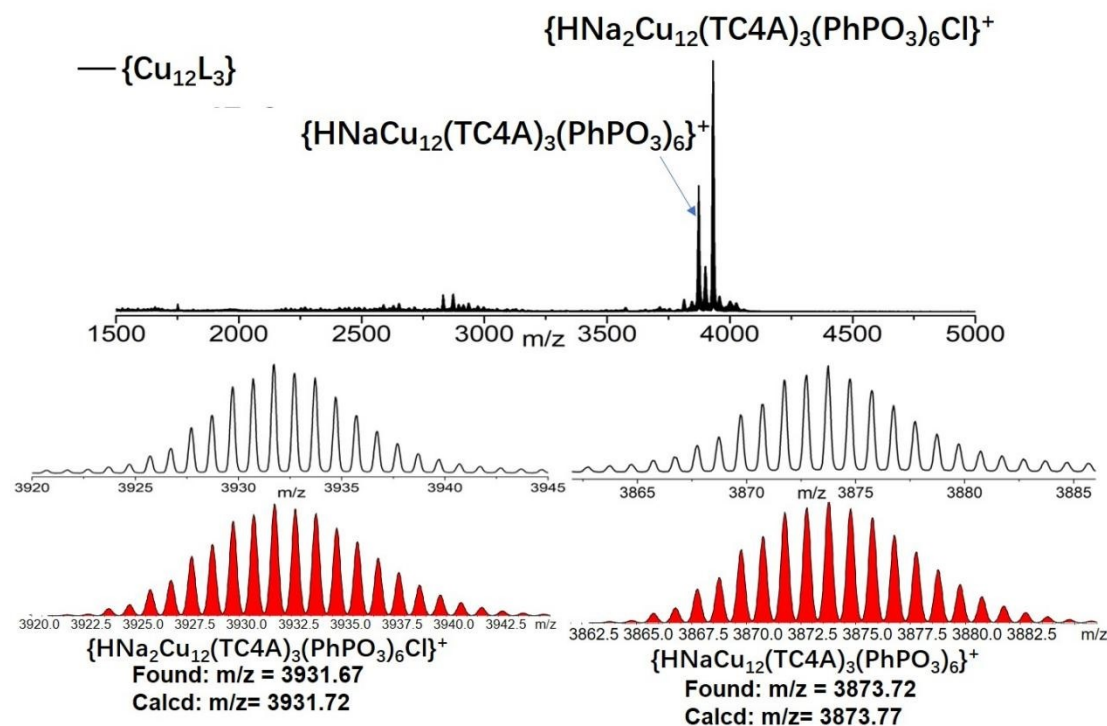
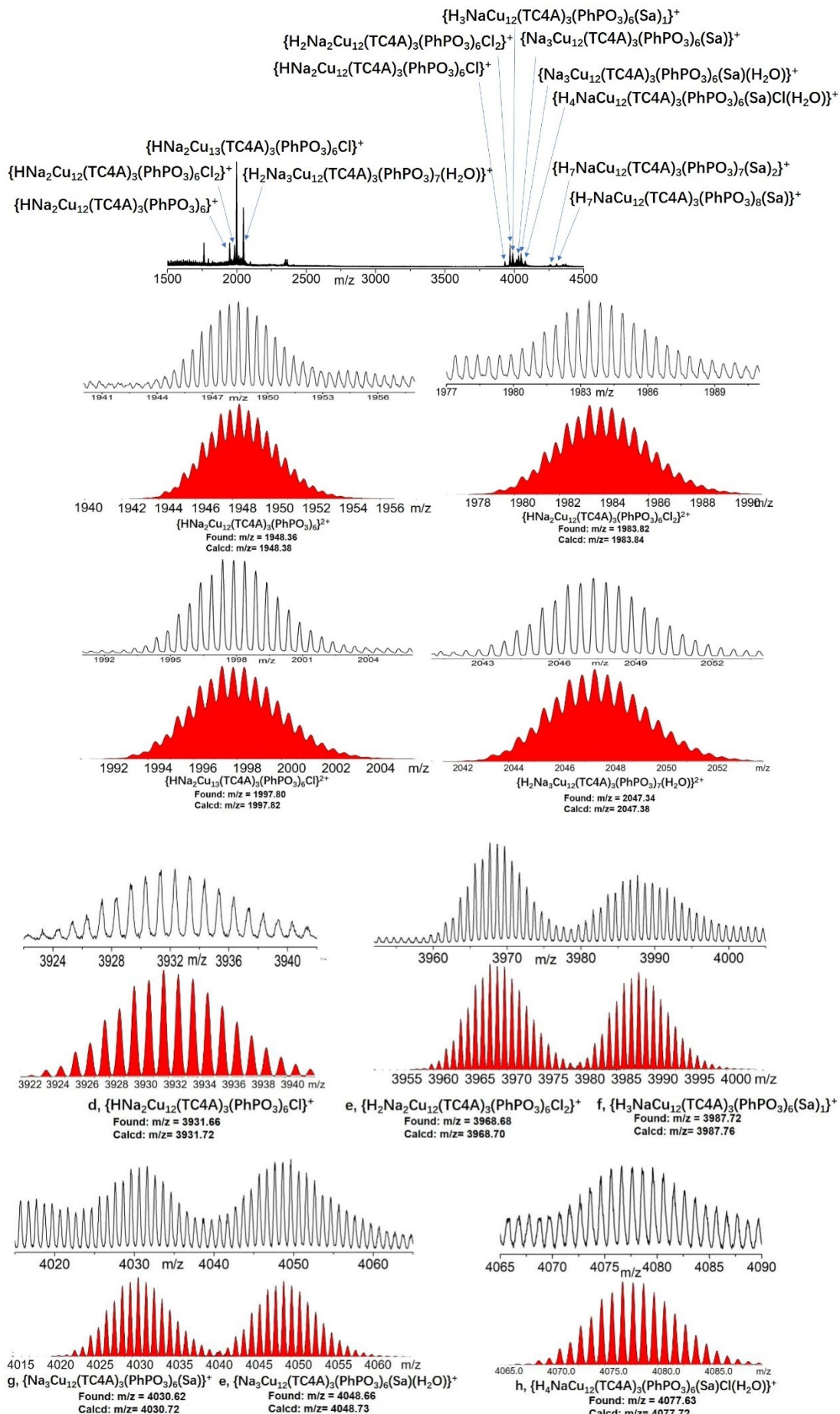


Figure S25. ESI-MS spectrum of the CH_2Cl_2 solution of Cu_{12}L_3 .



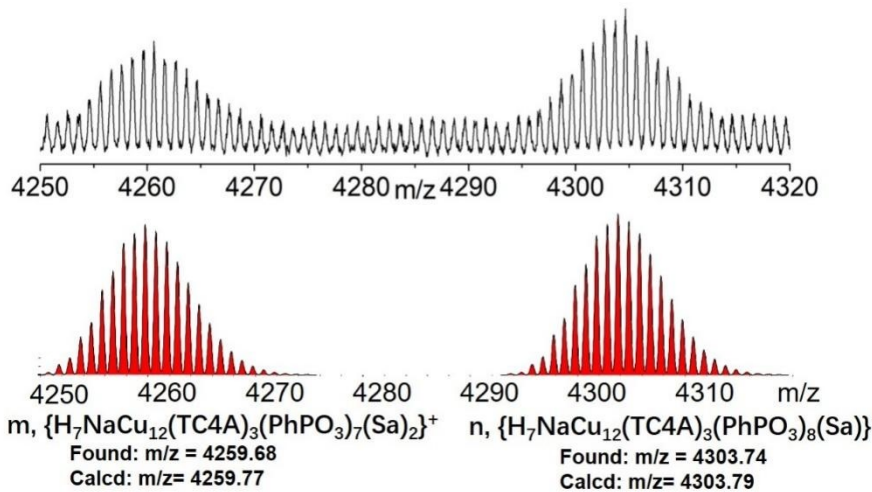


Figure S26. ESI-MS of reaction mixture of $Cu_{12}L_3$ and SaH_2 in $iPrOH/CH_2Cl_2$ solution.

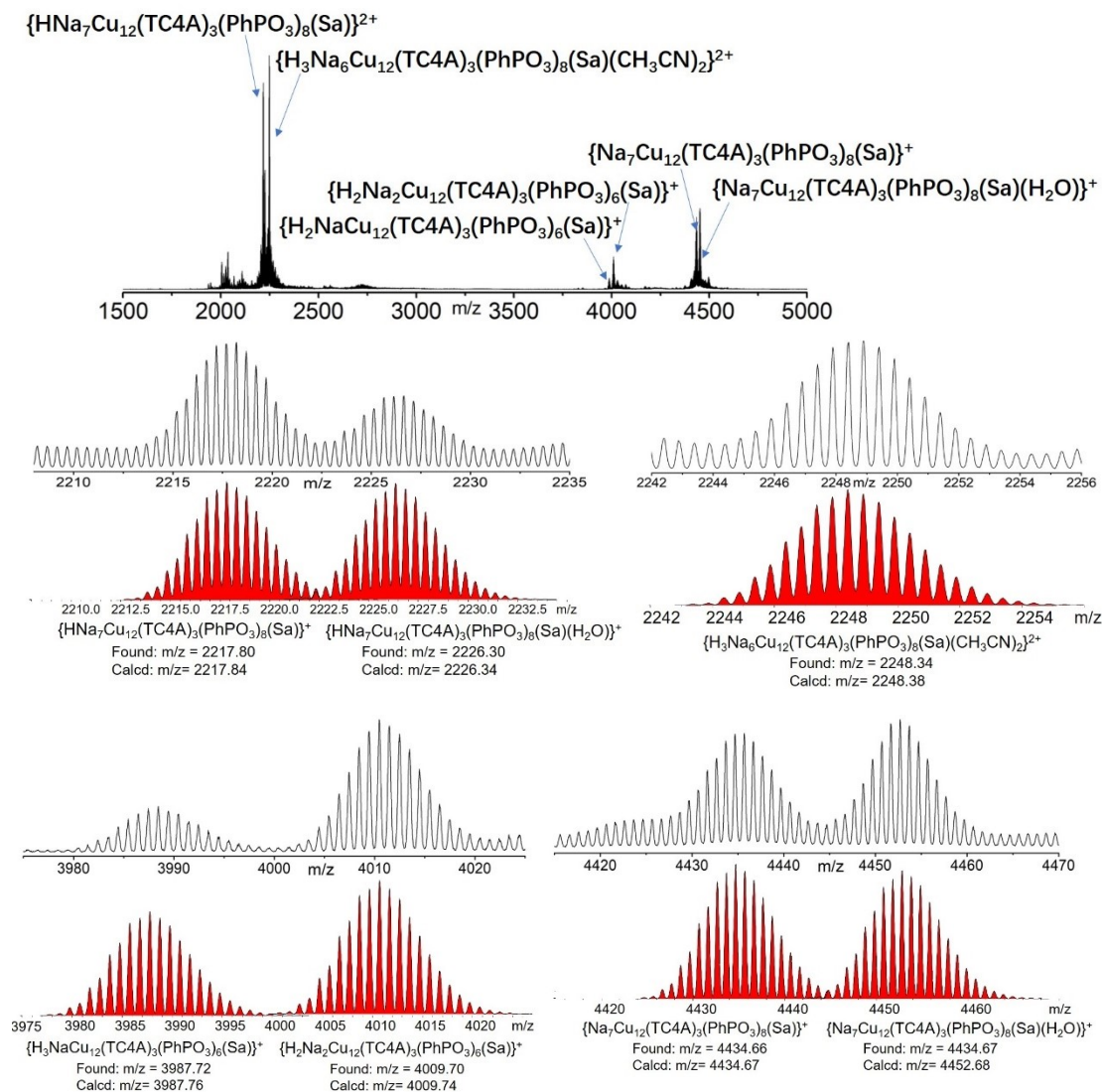


Figure S27. ESI-MS of CH_2Cl_2 solution of $Cu_{12}L_3$ - Sa .

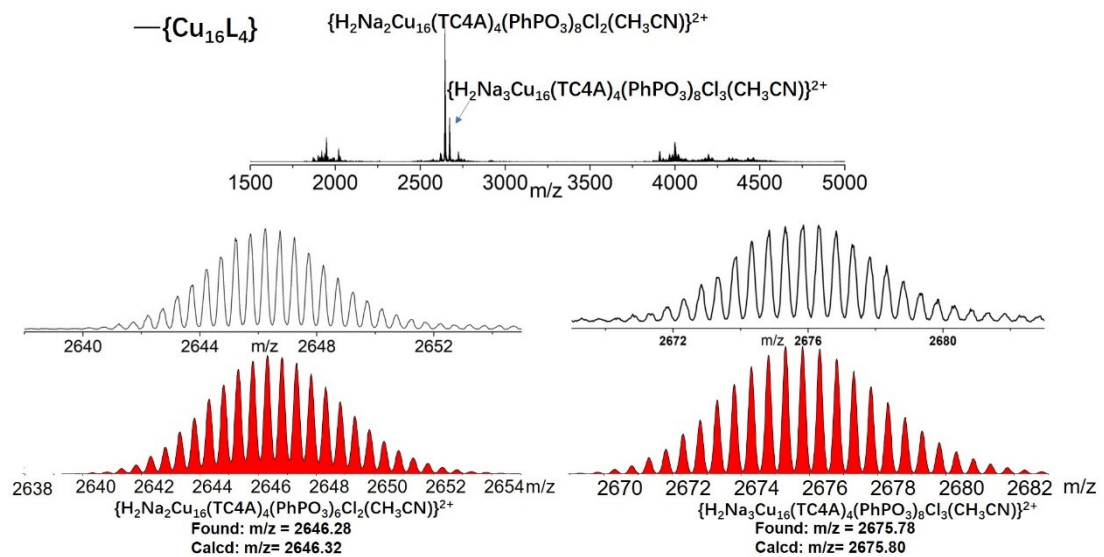


Figure S28. ESI-MS of CH₂Cl₂ solution of Cu₁₆L₄.

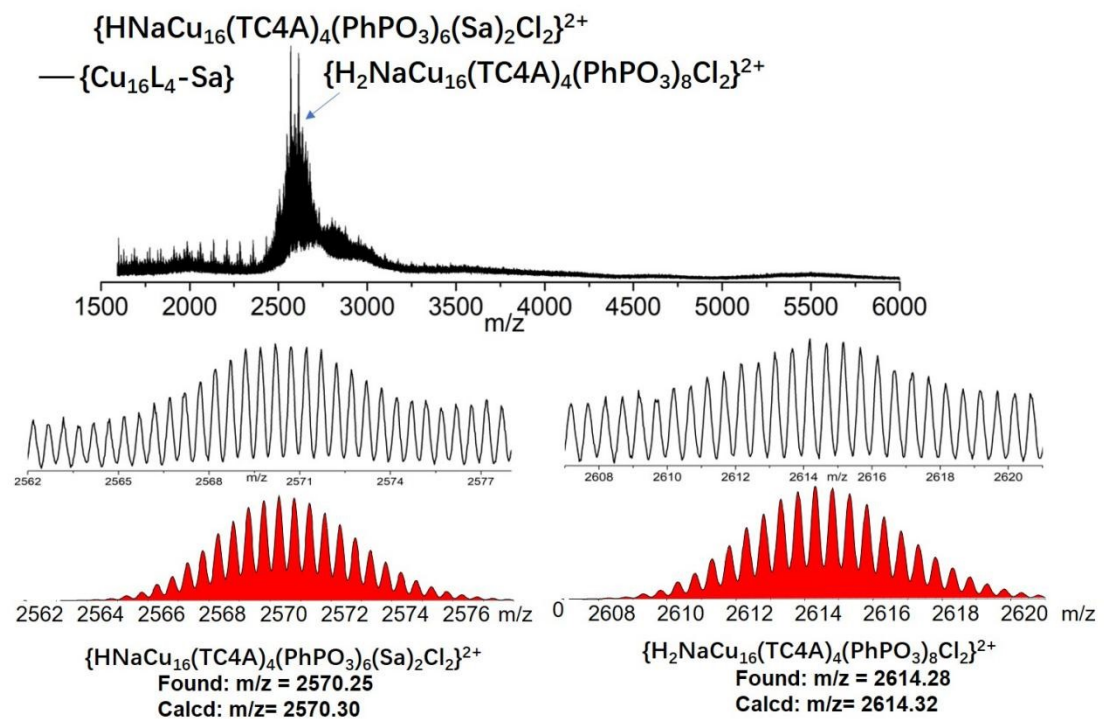


Figure S29. ESI-MS spectrum of the CH₂Cl₂ solution of Cu₁₆L₄-Sa.

10. Solid UV-Vis absorption spectra.

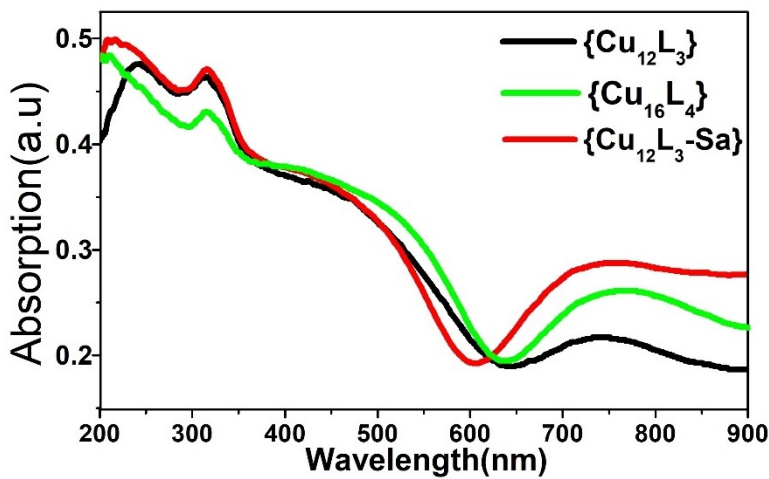


Figure S30. The solid UV-Vis absorption spectra of the clusters.

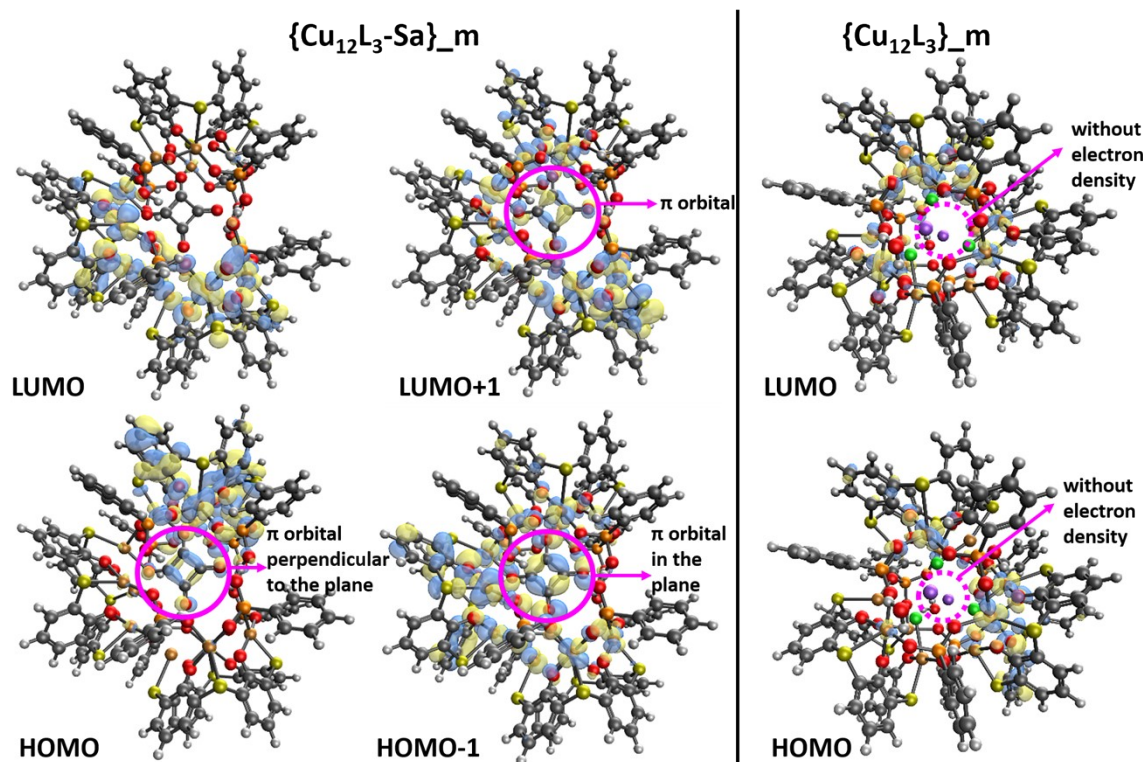
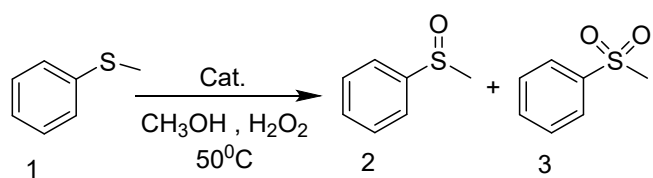


Figure S31. Related frontier molecular orbitals of $\{Cu_{12}L_3\}_m$ and $\{Cu_{12}L_3-Sa\}_m$.

11. Selective Sulfide Oxidation.

Table S2. Catalytic oxidation of phenyl methyl sulfide^a



Entry	Cat.	Oxidant	Solvent	Temp.(°C)	Time(h)	Conv.(%) ^c	Set.(%) ^d
1	Cu₁₆L₄	H ₂ O ₂	200uL	CH ₃ OH	50	1h	100
2	Cu₁₆L₄	H ₂ O ₂	180uL	CH ₃ OH	50	1h	88

3	Cu₁₆L₄	H ₂ O ₂	150uL	CH ₃ OH	50	1h	80	99
4	Cu₁₆L₄	H ₂ O ₂	100uL	CH ₃ OH	50	1h	58	99
5	Cu₁₆L₄	H ₂ O ₂	200uL	CH ₃ OH	40	1h	58	99
6	Cu₁₆L₄	H ₂ O ₂	200uL	CH ₃ OH	R.T.	1h	20	99
7	Cu₁₆L₄	H ₂ O ₂	200uL	CH ₃ CN	50	1h	57	77
8	Cu₁₆L₄	TBHP ^b	200uL	CH ₃ OH	50	1h	37	97
9	Cu₁₆L₄	TBHP	200uL	CH ₃ CN	50	1h	40	99
10	TC4A^c	H ₂ O ₂	200uL	CH ₃ OH	50	1h	20	99
11	PhPO₃H₂	H ₂ O ₂	200uL	CH ₃ OH	50	1h	26	99
12	CuCl	H ₂ O ₂	200uL	CH ₃ OH	50	1h	24	99
13	TC4A+PhPO₃H₂ + CuCl	H ₂ O ₂	200uL	CH ₃ OH	50	1h	44	99
14	none	H ₂ O ₂	200uL	CH ₃ OH	50	1h	20	99
15	Cu₁₆L₄	none		CH ₃ OH	50	1h	0	-

^a Reaction conditions: phenyl methy sulfide (0.7 mmol), catalyst (0.01 mmol%), oxidation (200 μ L);

^b TBHP = tert-butyl hydroperoxide;

^c conversion and selectivity were detected by ¹H NMR and GC;

^d selectivity = 2/(2+3);

^e TC4A=4-tert-butylthiacalix[4]arene

Table S3. Oxidative desulfurization of sulfide to sulfoxidea

Entry	Sulfide	Sulfoxide	Time	Cat.	Conv(%). ^b		Sel(%). ^c
					1 h	1h	
1			1 h	Cu ₁₂ L ₃	76.8	99	
				Cu ₁₂ L ₃ -Sa	78.3	99	
				Cu ₁₆ L ₄	100	99	
2			1h	Cu ₁₂ L ₃	74	100	
				Cu ₁₂ L ₃ -Sa	74	100	
				Cu ₁₆ L ₄	100	90	
3			1h	Cu ₁₂ L ₃	56	99	
				Cu ₁₂ L ₃ -Sa	54	99	
				Cu ₁₆ L ₄	100	99	
4			1h	Cu ₁₂ L ₃	58.27	99	
				Cu ₁₂ L ₃ -Sa	71.9	99	
				Cu ₁₆ L ₄	100	93.5	
5			1h	Cu ₁₂ L ₃	79	99	
				Cu ₁₂ L ₃ -Sa	70	99	
				Cu ₁₆ L ₄	100	95	
6			4h	Cu ₁₂ L ₃	39	99	
				Cu ₁₂ L ₃ -Sa	63.9	99	

			Cu_{16}L_4	96	99
7		2h	Cu_{12}L_3	31.5	99
			$\text{Cu}_{12}\text{L}_3\text{-Sa}$	23.8	99
			Cu_{16}L_4	100	99
8		0.25h	Cu_{12}L_3	50	99
			$\text{Cu}_{12}\text{L}_3\text{-Sa}$	52	99
			Cu_{16}L_4	100	99
9		0.75h	Cu_{12}L_3	73	99
			$\text{Cu}_{12}\text{L}_3\text{-Sa}$	77	99
			Cu_{16}L_4	100	99

[a] Reaction conditions: sulfide (0.7 mmol), catalyst (0.01 mmol%), oxidation (200 μL).

[b] conversion and selectivity were detected by ^1H NMR and GC.

[c]selectivity = 2/(2+3)

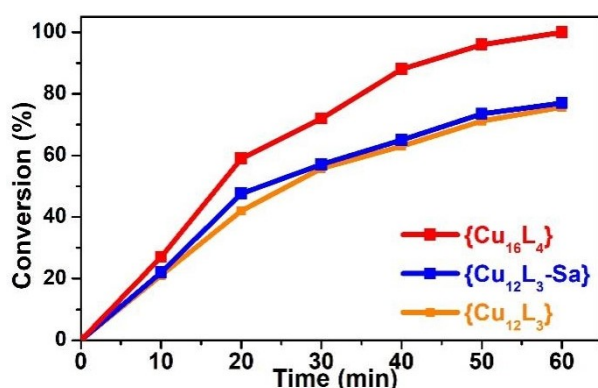


Figure S32. Time-conversion plot for the selective sulfide oxidation.

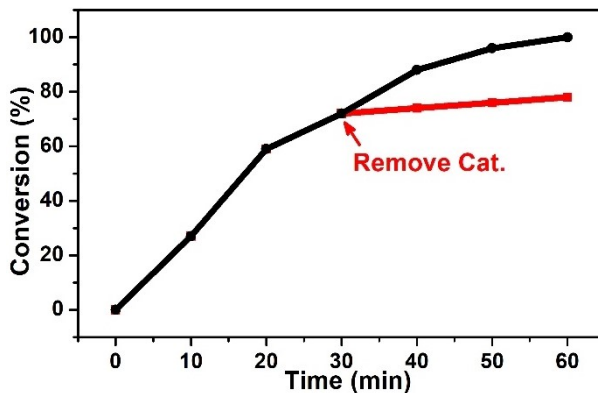


Figure S33. Time tracking and hot-filtration tests.

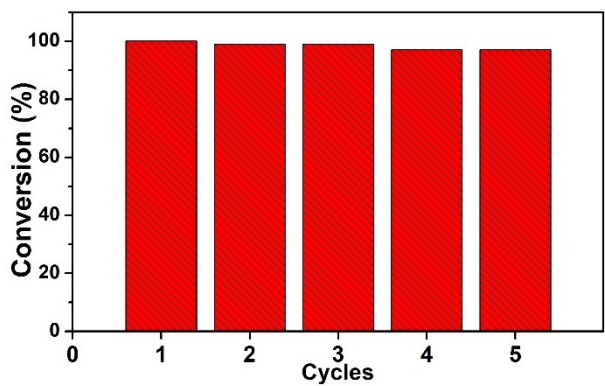


Figure S34. Recycling experiments of Cu_{16}L_4 .

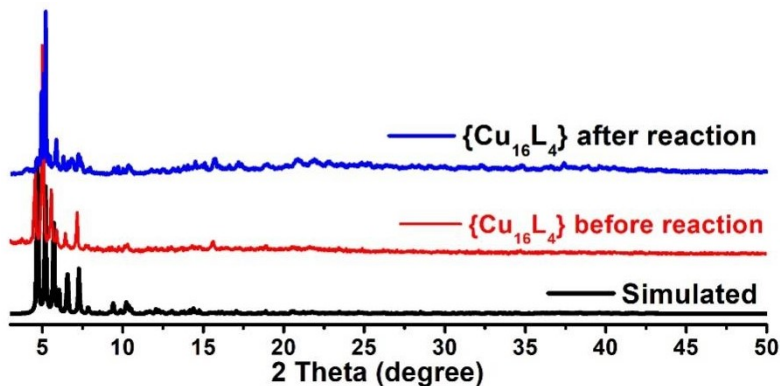


Figure S35. XRD of Cu_{16}L_4 before and after catalytic reaction.

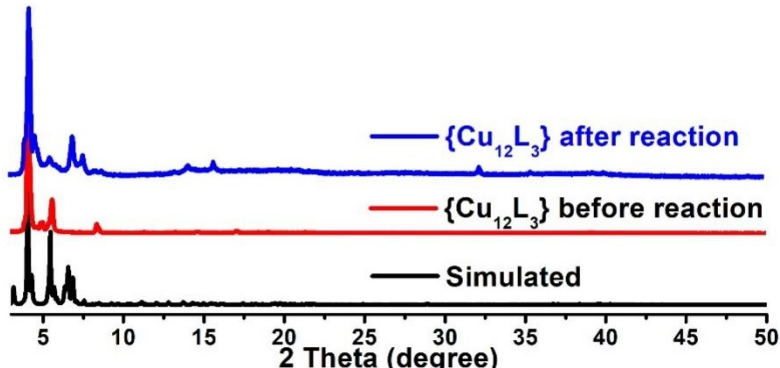


Figure S36. XRD of Cu_{16}L_4 before and after catalytic reaction.

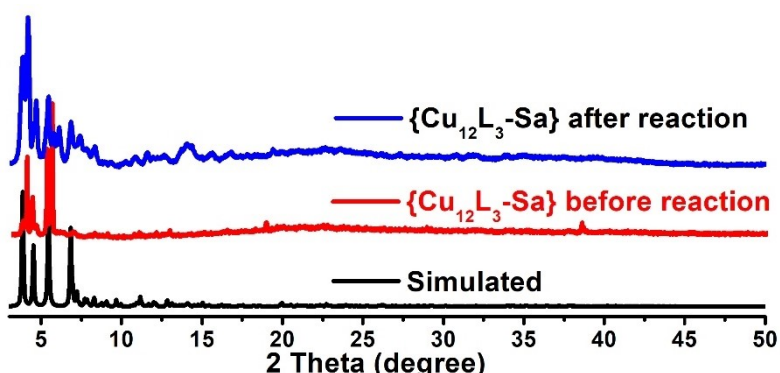


Figure S37. XRD of $\text{Cu}_{12}\text{L}_3\text{-Sa}$ before and after catalytic reaction.

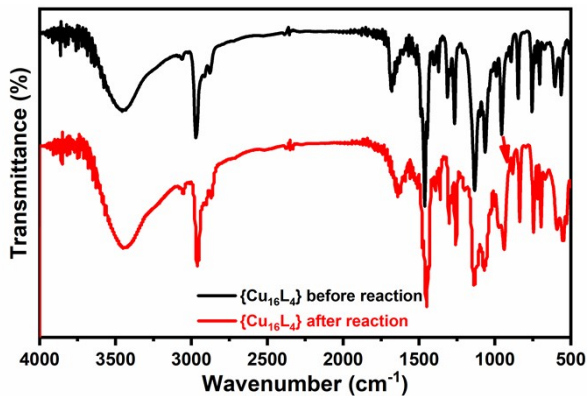


Figure S38. IR spectrum of Cu₁₆L₄ before and after catalytic reaction.

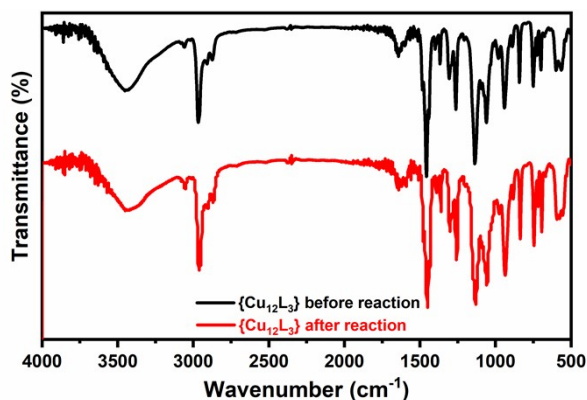


Figure S39. IR spectrum of Cu₁₂L₃ before and after catalytic reaction.

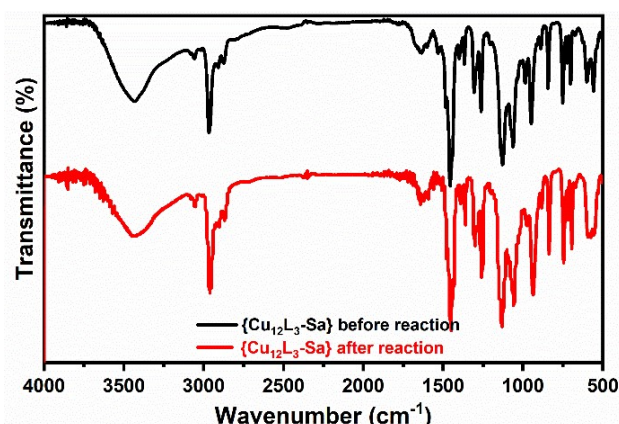


Figure S40. IR spectrum of Cu₁₂L₃-Sa before and after catalytic reaction.

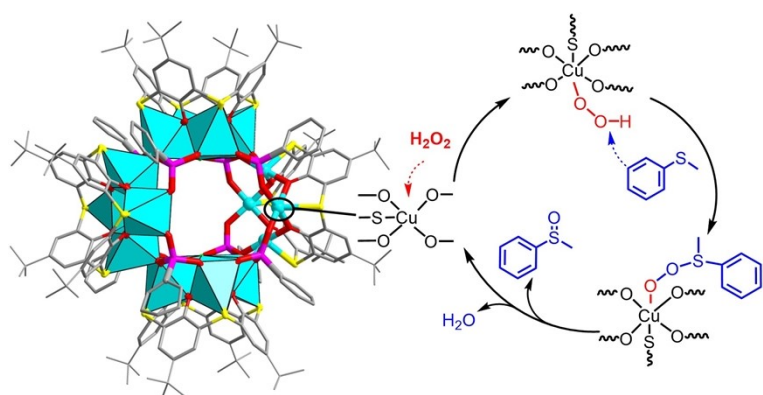


Figure S41. Possible catalytic mechanism for the oxidation of phenylmethyl sulfide.

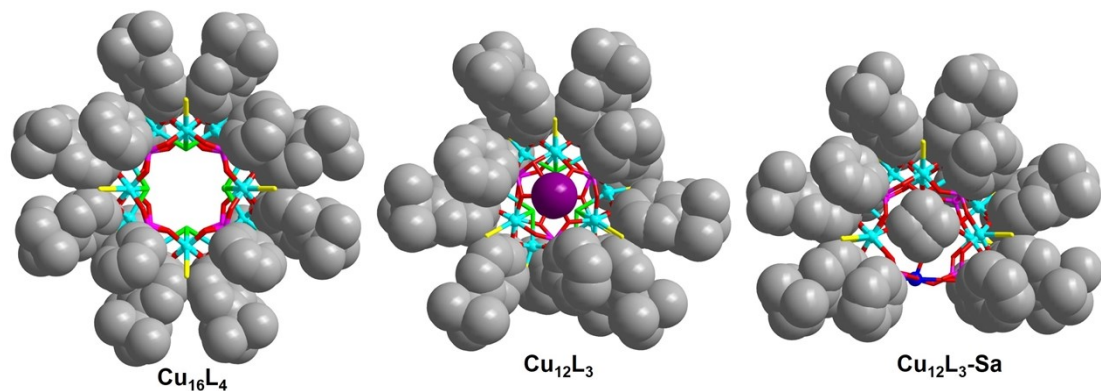


Figure S42. Space filling diagram of three structures.

12. BVS calculations

Table S4. BVS calculation for Cu_{12}L_3 and $\text{Cu}_{12}\text{L}_3\text{-Sa}$.

Cu_{12}L_3				$\text{Cu}_{12}\text{L}_3\text{-Sa}$			
Atom	Atom	Length/ \AA	S	Atom	Atom	Length/ \AA	S
Cu1	2.185			Cu1		2.141	
Cu1	Cl2	2.748	0.145	Cu1	S9	2.582	0.157
Cu1	S11	2.577	0.160	Cu1	O2	1.984	0.439
Cu1	O01I	1.941	0.493	Cu1	O9	1.928	0.510
Cu1	O01P	1.971	0.454	Cu1	O32	1.861	0.611
Cu1	O012	1.952	0.478	Cu1	O33	1.997	0.423
Cu1	O013	1.970	0.455				
Cu2	2.127			Cu2		2.135	
Cu2	Cl2	2.574	0.232	Cu2	S8	2.615	0.144
Cu2	S12	2.625	0.140	Cu2	O7	1.982	0.441
Cu2	O01C	1.994	0.427	Cu2	O14	1.951	0.479
Cu2	O01D	1.992	0.429	Cu2	O27	1.984	0.439
Cu2	O013	1.967	0.459	Cu2	O30	2.371	0.154
Cu2	O018	1.983	0.440	Cu2	O31	1.952	0.478
Cu3	2.269			Cu3		2.079	
Cu3	Cl2	2.745	0.146	Cu3	S12	2.566	0.164
Cu3	S10	2.588	0.155	Cu3	O3	2.006	0.413
Cu3	O01N	1.904	0.544	Cu3	O6	1.959	0.469
Cu3	O01R	1.923	0.517	Cu3	O13	1.907	0.540
Cu3	O015	1.960	0.468	Cu3	O18	1.941	0.493
Cu3	O018	1.984	0.439				
Cu4	2.141			Cu4		1.880	
Cu4	Cl2	2.516	0.271	Cu4	S5	2.599	0.150
Cu4	S9	2.614	0.144	Cu4	O20	1.999	0.421
Cu4	O010	2.005	0.414	Cu4	O28	2.027	0.390
Cu4	O012	1.997	0.423	Cu4	O38	1.996	0.425

Cu4	O015	1.963	0.464	Cu4	O39	1.940	0.494
Cu4	O019	1.997	0.423				
Cu5	2.137			Cu5	1.922		
Cu5	Cl3	2.515	0.272	Cu5	S2	2.547	0.173
Cu5	S8	2.597	0.151	Cu5	O8	2.013	0.405
Cu5	O010	1.975	0.449	Cu5	O22	1.997	0.423
Cu5	O014	1.993	0.428	Cu5	O26	1.940	0.494
Cu5	O016	1.980	0.443	Cu5	O31	1.995	0.426
Cu5	O019	2.024	0.394				
Cu6	2.140			Cu6	2.174		
Cu6	Cl3	2.766	0.138	Cu6	S11	2.545	0.174
Cu6	S7	2.574	0.161	Cu6	O4	1.923	0.517
Cu6	O01H	1.979	0.444	Cu6	O19	1.875	0.589
Cu6	O01S	1.913	0.531	Cu6	O33	1.957	0.472
Cu6	O2	2.009	0.410	Cu6	O38	1.998	0.422
Cu6	O016	1.970	0.455				
Cu7	2.096			Cu7	2.004		
Cu7	Cl3	2.569	0.235	Cu7	S1	2.624	0.140
Cu7	S5	2.618	0.143	Cu7	O3	1.952	0.478
Cu7	O01A	2.001	0.419	Cu7	O10	1.986	0.436
Cu7	O01B	2.000	0.420	Cu7	O23	1.942	0.491
Cu7	O01H	1.976	0.448	Cu7	O25	1.968	0.458
Cu7	O017	1.990	0.431				
Cu8	2.196			Cu8	2.098		
Cu8	Cl3	2.767	0.138	Cu8	S4	2.568	0.164
Cu8	S6	2.577	0.160	Cu8	O12	1.925	0.514
Cu8	O01G	1.912	0.533	Cu8	O16	1.914	0.530
Cu8	O01Q	1.985	0.437	Cu8	O23	1.985	0.437
Cu8	O014	1.956	0.473	Cu8	O29	1.972	0.453
Cu8	O017	1.970	0.455				
Cu9	2.109			Cu9	2.069		
Cu9	Cl1	2.525	0.265	Cu9	S3	2.567	0.164
Cu9	S4	2.621	0.142	Cu9	O14	1.975	0.449
Cu9	O01A	1.995	0.426	Cu9	O15	1.931	0.506
Cu9	O01B	1.997	0.423	Cu9	O24	2.000	0.420
Cu9	O01E	1.989	0.433	Cu9	O40	1.914	0.530
Cu9	O01J	1.999	0.421				
Cu10	1.998			Cu10	2.142		
Cu10	S1	2.557	0.168	Cu10	S10	2.599	0.151
Cu10	O01J	1.980	0.443	Cu10	O2	1.982	0.441
Cu10	O01K	1.952	0.478	Cu10	O10	1.978	0.446
Cu10	O01M	1.964	0.463	Cu10	O20	1.916	0.527
Cu10	O011	1.978	0.446	Cu10	O25	1.991	0.430
				Cu10	O34	2.388	0.147

Cu11	2.134			Cu11	2.109		
Cu11	C11	2.532	0.260	Cu11	S7	2.542	0.175
Cu11	S2	2.627	0.139	Cu11	O5	1.890	0.565
Cu11	O01C	1.998	0.422	Cu11	O22	1.969	0.457
Cu11	O01D	1.993	0.428	Cu11	O24	2.014	0.404
Cu11	O01F	1.998	0.422	Cu11	O36	1.930	0.507
Cu11	O011	1.964	0.463				
Cu12	2.083			Cu12	1.982		
Cu12	S3	2.568	0.164	Cu12	S6	2.579	0.159
Cu12	O01E	1.984	0.439	Cu12	O6	1.977	0.447
Cu12	O01F	1.963	0.464	Cu12	O7	1.982	0.441
Cu12	O01L	1.940	0.494	Cu12	O27	1.959	0.469
Cu12	O01O	1.919	0.523	Cu12	O29	1.961	0.467
$R_0(\text{Cu-Cl})=2.033$		$R_0(\text{Cu-S})=1.898$		$R_0(\text{Cu-O})=1.679$			

Table S5. BVS calculation for $\{\text{Cu}_{16}\text{L}_4\}$ and $\{\text{Cu}_{16}\text{L}_4\text{-Sa}\}$.

$\{\text{Cu}_{16}\text{L}_4\}$				$\{\text{Cu}_{16}\text{L}_4\text{-Sa}\}$			
Atom	Atom	Length/Å	S	Atom	Atom	Length/Å	S
Cu1	2.122			Cu1	1.975		
Cu1	Cl0L	2.619	0.205	Cu1	S00G	2.589	0.154
Cu1	S00F	2.625	0.140	Cu1	Cl0K	2.594	0.220
Cu1	O00T	1.964	0.463	Cu1	O71	1.967	0.459
Cu1	O00W	1.977	0.447	Cu1	O70	2.070	0.348
Cu1	O00Y	1.980	0.443	Cu1	O71	1.983	0.440
Cu1	O011	1.997	0.423	Cu1	O79	2.063	0.354
Cu2	2.096			Cu2	2.098		
Cu2	Cl0L	2.674	0.177	Cu2	S00A	2.632	0.137
Cu2	S00I	2.613	0.145	Cu2	Cl0K	2.718	0.157
Cu2	O00T	1.975	0.449	Cu2	O00N	1.995	0.426
Cu2	O00U	2.021	0.397	Cu2	O71	1.994	0.427
Cu2	O015	1.989	0.433	Cu2	O67	1.940	0.494
Cu2	O62	1.939	0.495	Cu2	O012	1.969	0.457
Cu3	2.108			Cu3	2.112		
Cu3	Cl0L1	2.610	0.210	Cu3	S00B	2.628	0.139
Cu3	S00D1	2.671	0.124	Cu3	Cl0K	2.715	0.158
Cu3	O00U1	1.991	0.430	Cu3	O00N	1.968	0.458
Cu3	O00V	2.014	0.404	Cu3	O00Q	1.979	0.444
Cu3	O601	1.943	0.490	Cu3	O661	1.970	0.455
Cu3	O61	1.975	0.449	Cu3	O72	1.969	0.457
Cu4	2.157			Cu4	2.108		
Cu4	Cl0M	2.568	0.236	Cu4	S00E1	2.612	0.145
Cu4	S00B	2.638	0.135	Cu4	Cl0I1	2.728	0.153
Cu4	O00N	2.008	0.411	Cu4	O00M1	2.014	0.404
Cu4	O00O	2.014	0.404	Cu4	O00O1	1.990	0.431
Cu4	O63	1.944	0.489	Cu4	O63	1.957	0.472

Cu4	O64	1.949	0.482	Cu4	O68	1.934	0.502
Cu5	2.121			Cu5	2.277		
Cu5	Cl0M	2.661	0.183	Cu5	Cl0K1	2.599	0.217
Cu5	S00C	2.611	0.146	Cu5	S00L1	2.638	0.135
Cu5	O00N	1.980	0.443	Cu5	O721	1.989	0.433
Cu5	O00P	1.957	0.472	Cu5	O791	1.993	0.428
Cu5	O00W	1.965	0.462	Cu5	O64	1.921	0.520
Cu5	O011	2.004	0.415	Cu5	O8	1.904	0.544
Cu6	2.145			Cu6	2.034		
Cu6	Cl0M	2.566	0.237	Cu6	S00H	2.603	0.149
Cu6	S00A	2.664	0.126	Cu6	Cl0I	2.567	0.236
Cu6	O00P	1.993	0.428	Cu6	O00M	2.022	0.396
Cu6	O00Q	2.013	0.405	Cu6	O00S	1.954	0.476
Cu6	O016	1.976	0.448	Cu6	O701	1.966	0.460
Cu6	O651	1.935	0.501	Cu6	O7	2.103	0.318
Cu7	2.077			Cu7	2.215		
Cu7	Cl0M	2.707	0.162	Cu7	Cl0I	2.651	0.188
Cu7	S009	2.611	0.146	Cu7	S00J	2.607	0.147
Cu7	O00O	1.951	0.479	Cu7	O00R	1.993	0.428
Cu7	O00Q	1.996	0.425	Cu7	O00S	2.001	0.419
Cu7	O00V	1.970	0.455	Cu7	O80	1.918	0.524
Cu7	O61	2.009	0.410	Cu7	O6	1.929	0.509
Cu8	2.097			Cu8	2.109		
Cu8	Cl0L	2.690	0.169	Cu8	S009	2.628	0.139
Cu8	S00K	2.632	0.137	Cu8	Cl0I	2.726	0.154
Cu8	O00Y	2.010	0.409	Cu8	O00O	1.950	0.481
Cu8	O010	1.947	0.485	Cu8	O00Q	1.992	0.429
Cu8	O014	1.948	0.483	Cu8	O00R	1.975	0.449
Cu8	O60	2.006	0.413	Cu8	O661	1.969	0.457
$R_0(\text{Cu-Cl})=2.033$		$R_0(\text{Cu-S})=1.898$		$R_0(\text{Cu-O})=1.679$			